

## Solution Conformations of Dodecasubstituted Cobalt(II) Porphyrins

Craig J. Medforth,<sup>\*,†</sup> J. David Hobbs,<sup>‡</sup> Marisol R. Rodriguez,<sup>†</sup> Raymond J. Abraham,<sup>§</sup> Kevin M. Smith,<sup>\*,†</sup> and John A. Shelnutt<sup>\*,‡</sup>

Department of Chemistry, University of California, Davis, California 95616, Fuel Science Department, Sandia National Laboratories, Albuquerque, New Mexico 87185-0710, and Department of Chemistry, University of Liverpool, P.O. Box 147, Liverpool, L69 3BX, U.K.

Received March 31, 1994<sup>Ⓢ</sup>

The solution conformations of seven dodecasubstituted porphyrins, which generally show extremely nonplanar structures in the crystalline state, have been investigated using a method that combines proton NMR spectroscopy and molecular mechanics calculations. By comparison of the proton paramagnetic shifts measured for cobalt(II) complexes of these porphyrins with the dipolar shifts calculated using geometric factors obtained either from crystallographic data or from molecular mechanics structures, it is determined that the conformations of the macrocycles and their substituents are similar in solution and in the crystalline state. Thus, the nonplanar cobalt(II) porphyrins that have well-defined cavity structures in the crystalline state retain these cavities in solution. Variable-temperature proton NMR spectroscopy is used to estimate the dynamic stabilities of the cavity structures. The porphyrins with cavities are found to behave differently from planar porphyrins without cavities with regard to the formation of  $\pi$ -complexes with 1,3,5-trinitrobenzene. It is suggested that the cavities may modulate a range of porphyrin–substrate interactions, potentially making these porphyrins useful as regio- and stereoselective oxidation catalysts and in the preparation of complexes with well-defined ligand orientations.

## Introduction

Recent studies<sup>1–23</sup> have shown that dodecasubstituted porphyrins such as **1**,<sup>1–8</sup> **2**,<sup>9–12</sup> **3**,<sup>13–16</sup> **4**,<sup>17,18</sup> **5**,<sup>14</sup> and **6**<sup>4,7,19,20</sup> adopt

highly nonplanar conformations in order to minimize steric repulsions between the peripheral substituents. These nonplanar conformations give rise to many unusual structural, spectroscopic, and chemical properties.<sup>24</sup> Although it is known that dodecasubstituted porphyrins such as **1b,c** retain highly nonplanar conformations in solution,<sup>3b,4,5,7</sup> it is not certain whether these conformations are the same as those determined crystallographically.<sup>3b,5,7</sup> In this work, the solution conformations of porphyrins **1b,c** and several other dodecasubstituted porphyrins are investigated in detail.

A specific aim of this work is to determine whether the cavity structures observed crystallographically for porphyrins **1b,c** (Figure 2) are retained in solution. Porphyrins with cavity structures are of interest because they may possess several useful properties. For example, they might provide regio- and ste-

<sup>†</sup> University of California.

<sup>‡</sup> Sandia National Laboratories.

<sup>§</sup> University of Liverpool.

<sup>Ⓢ</sup> Abstract published in *Advance ACS Abstracts*, January 1, 1995.

- (1) Dolphin, D. J. *Heterocycl. Chem.* **1970**, *7*, 275.
- (2) Evans, B.; Smith, K. M.; Fuhrhop, J.-H. *Tetrahedron Lett.* **1977**, *5*, 443.
- (3) (a) Barkigia, K. M.; Chantranupong, L.; Smith, K. M.; Fajer, J. J. *Am. Chem. Soc.* **1988**, *110*, 7566. (b) Barkigia, K. M.; Berber, M. D.; Fajer, J.; Medforth, C. J.; Renner, M. W.; Smith, K. M. *J. Am. Chem. Soc.* **1990**, *112*, 8851.
- (4) Shelnutt, J. A.; Medforth, C. J.; Berber, M. D.; Barkigia, K. M.; Smith, K. M. *J. Am. Chem. Soc.* **1991**, *113*, 4077.
- (5) Sparks, L. D.; Medforth, C. J.; Park, M.-S.; Chamberlain, J. R.; Ondrias, M. R.; Senge, M. O.; Smith, K. M.; Shelnutt, J. A., *J. Am. Chem. Soc.* **1993**, *115*, 581.
- (6) (a) Shelnutt, J. A.; Majumder, S. A.; Sparks, L. D.; Hobbs, J. D.; Medforth, C. J.; Senge, M. O.; Smith, K. M.; Miura, M.; Luo, L.; Quirke, J. M. E. *J. Raman Spectrosc.* **1992**, *23*, 523. (b) Stichternath, A.; Schweitzer-Stenner, R.; Dreybrodt, W.; Mak, R. S. W.; Li, X.-Y.; Sparks, L. D.; Shelnutt, J. A.; Medforth, C. J.; Smith, K. M. *J. Phys. Chem.* **1993**, *97*, 3701. (c) Anderson, K. K.; Hobbs, J. D.; Luo, L.; Stanley, K. D.; Quirke, J. M. E.; Shelnutt, J. A. *J. Am. Chem. Soc.* **1993**, *115*, 12346. (d) Sparks, L. D.; Anderson, K. K.; Medforth, C. J.; Smith, K. M.; Shelnutt, J. A. *Inorg. Chem.* **1994**, *33*, 2297.
- (7) Barkigia, K. M.; Renner, M. W.; Furenliid, L. R.; Medforth, C. J.; Smith, K. M.; Fajer, J. *J. Am. Chem. Soc.* **1993**, *115*, 3627.
- (8) (a) Kadish, K. M.; Caemelbecke, E. V.; D'Souza, F.; Medforth, C. J.; Smith, K. M.; Tabard, A.; Guillard, R. *Organometallics* **1993**, *12*, 2411. (b) Kadish, K. M.; Caemelbecke, E. V.; Boulas, P.; D'Souza, F.; Vogel, E.; Kisters, M.; Medforth, C. J.; Smith, K. M. *Inorg. Chem.* **1993**, *32*, 4177.
- (9) (a) Traylor, T. G.; Tsuchiya, S. *Inorg. Chem.* **1987**, *26*, 1338. (b) Tsuchiya, S.; Seno, M. *Chem. Lett.* **1989**, 263.
- (10) (a) Bhyrappa, P.; Krishnan, V. *Inorg. Chem.* **1991**, *30*, 239. (b) Bhyrappa, P.; Nethaji, M.; Krishnan, V. *Chem. Lett.* **1993**, 871. (c) Bhyrappa, P.; Krishnan, V.; Nethaji, M. *J. Chem. Soc., Dalton Trans.* **1993**, 1901.
- (11) Lyons, J. E.; Ellis, P. E., Jr.; Wagner, R. W.; Thompson, P. B.; Gray, H. B.; Hughes, M. E.; Hodge, J. A. *ACS Div. Petroleum Chem. Prepr.* **1992**, *37*, 307 and references therein.
- (12) Mandon, D.; Ochsenein, P.; Fischer, J.; Weiss, R.; Jayaraj, K.; Gold, A.; White, P. S.; Brigaud, O.; Battioni, P.; Mansuy, D. *Inorg. Chem.* **1992**, *31*, 2044.
- (13) Medforth, C. J.; Smith, K. M. *Tetrahedron Lett.* **1990**, *31*, 5583.
- (14) Medforth, C. J.; Senge, M. O.; Smith, K. M.; Sparks, L. D.; Shelnutt, J. A. *J. Am. Chem. Soc.* **1992**, *114*, 9859.
- (15) (a) Tsuchiya, S. *Chem. Phys. Lett.* **1990**, 608. (b) Tsuchiya, S. *J. Chem. Soc., Chem. Commun.* **1991**, 716. (c) Tsuchiya, S. *J. Chem. Soc., Chem. Commun.* **1992**, 1475.
- (16) (a) Takeda, J.; Ohya, T.; Sato, M. *Chem. Phys. Lett.* **1991**, *183*, 384. (b) Takeda, J.; Ohya, T.; Sato, M. *Inorg. Chem.* **1992**, *31*, 2877.
- (17) (a) Wu, G.-Z.; Gan, W.-X.; Leung, H.-K. *J. Chem. Soc., Faraday Trans.* **1991**, *87*, 2933. (b) Senge, M. O. *J. Chem. Soc., Dalton Trans.* **1993**, 3539.
- (18) Zhu, N.-J.; Li, Y.; Wu, G.-Z.; Liang, X.-G. *Acta Chim. Sinica* **1992**, *50*, 249.
- (19) Medforth, C. J.; Berber, M. D.; Smith, K. M.; Shelnutt, J. A. *Tetrahedron Lett.* **1990**, *31*, 3719.
- (20) Senge, M. O.; Medforth, C. J.; Sparks, L. D.; Smith, K. M.; Shelnutt, J. A. *Inorg. Chem.* **1993**, *32*, 1716.
- (21) Remy, D. E. *Tetrahedron Lett.* **1983**, *24*, 1451.
- (22) Renner, M. W.; Cheng, R.-J.; Chang, C. K.; Fajer, J. *J. Phys. Chem.* **1990**, *94*, 8508.
- (23) Cheng, R.-J.; Chen, Y.-R.; Chuang, C.-E. *Heterocycles* **1992**, *34*, 1.
- (24) The uses of highly nonplanar porphyrins in evaluating the effects of nonplanarity in biological systems have recently been reviewed: (a) Fajer, J.; Barkigia, K. M.; Smith, K. M.; Zhong, E.; Gudowska-Nowak, E.; Newton, M. In *Reaction Centers of Photosynthetic Bacteria*; Michel-Beyerle, M. E., Ed.; Springer-Verlag: Berlin, 1990; p 367. (b) Fajer, J. *Chem. Ind.* **1991**, 869. (c) Senge, M. O. *J. Photochem. Photobiol. B: Biol.* **1992**, *16*, 3.

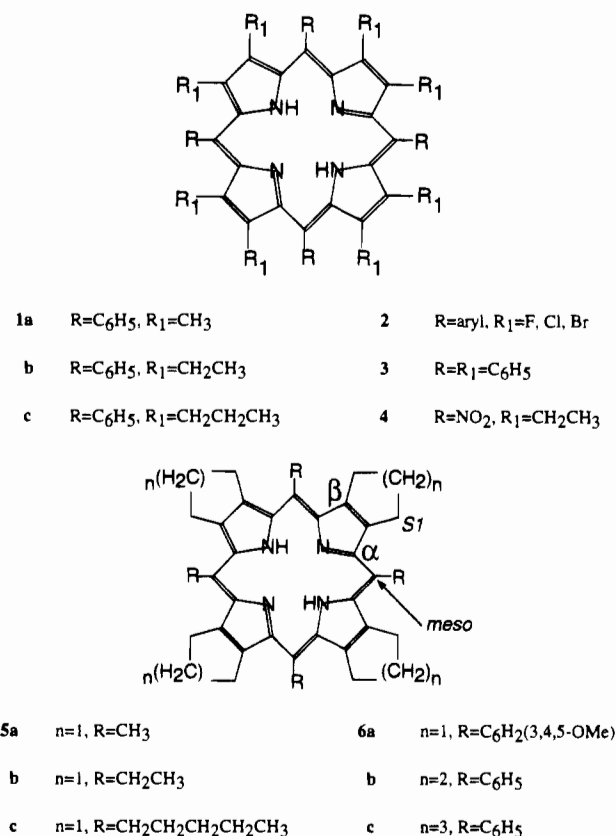


**Figure 1.** Structures of some dodecasubstituted porphyrins and the nomenclature used for labeling the porphyrin atoms. The solution conformations of cobalt(II) complexes of porphyrins **1a–c**, **3**, and **6a–c** (abbreviated to **Co1a–c**, **Co3**, and **Co6a–c**) are investigated in this study.

reoselectivity, as well as protection from oxidative degradation, in oxidation reactions designed to mimic cytochrome P-450.<sup>25</sup> In this light, it is interesting to note that a derivative of **3** is proposed to form an unusually stable oxo-iron(IV) radical cation.<sup>15b</sup> Metal complexes of **2** have also been found to be robust alkane oxidation catalysts.<sup>11</sup> Further, the orientation of the axial histidine ligand is believed to be one mechanism for modulating the spectroscopic and redox properties of heme proteins,<sup>26</sup> and numerous attempts have been made to prepare porphyrins with specific ligand orientations.<sup>26–30</sup> Porphyrins with groove-like cavity structures might allow the preparation of complexes with specific ligand orientations governed by the conformation of the porphyrin and its substituents.

To utilize these cavity effects, detailed information about the solution conformations of dodecasubstituted porphyrins is required. In this work, molecular mechanics calculations and proton NMR spectroscopy are used in combination to investigate the solution conformations of cobalt(II) complexes of the dodecasubstituted porphyrins **1a–c**, **3**, and **6a–c** (abbreviated

as **Co1a–c**, **Co3**, and **Co6a–c**). A preliminary study is also made of the effects of nonplanarity and the presence of a cavity on the interactions of these porphyrins with small molecules.

## Materials and Methods

**Synthesis of Porphyrins.** Porphyrins **1a–c**, **3**, and **6a–c** were synthesized as described previously.<sup>3b,4,13,19,20</sup> Cobalt(II) complexes were typically prepared using a minor modification of the standard metal acetate procedure.<sup>31</sup> Porphyrin (50 mg) was dissolved in chloroform (20 mL) and the mixture brought to reflux under nitrogen, whereupon 1 mL of a saturated solution of cobalt(II) acetate in methanol was added using a syringe. The reaction was followed spectrophotometrically until metal insertion was complete. The reaction mixture was cooled, washed with water (2 × 50 mL), and filtered through anhydrous sodium sulfate, and the chloroform was removed under vacuum. Addition of methanol to a solution of the porphyrin in methylene chloride caused the porphyrin to crystallize or precipitate out of solution, whereupon the porphyrin was filtered off and dried under vacuum at 40 °C for 12 h. Nickel(II) complexes were prepared and purified using the procedures described previously.<sup>4,20</sup>

**Proton NMR Studies.** Proton NMR spectra were typically measured at a spectrometer frequency of 300 MHz, using 0.005 M solutions of the cobalt(II) and nickel(II) porphyrins at a temperature of 298 K. The solvent peak was used as an internal standard at 7.26 ppm (CDCl<sub>3</sub>), 7.16 ppm (C<sub>6</sub>D<sub>6</sub>), 5.94 ppm (CDCl<sub>2</sub>CDCl<sub>2</sub>), 5.30 ppm (CD<sub>2</sub>Cl<sub>2</sub>), 2.62 ppm (CD<sub>3</sub>SOCD<sub>3</sub>), and 2.09 ppm (C<sub>6</sub>D<sub>5</sub>CD<sub>3</sub>). TMS was used as an internal standard in CCl<sub>4</sub>. The variable-temperature unit was calibrated using a sample of methanol.<sup>32</sup>

**Molecular Modeling Calculations.** Molecular mechanics calculations using POLYGRAF software (Molecular Simulations Inc.) were carried out and displayed on a Silicon Graphics 4D210 Power Series or 4D35 Personal Iris workstation. The force constants used in the molecular mechanics forcefield were obtained from a normal coordinate analysis of NiOEP<sup>33a–c</sup> and the DREIDING force field,<sup>33d</sup> and equilibrium bond distances, angles, torsions, and inversions were adjusted to reproduce the crystal structure of planar, triclinic B NiOEP.<sup>34</sup> The force field used in the calculations is known to accurately reproduce the crystal structures of various dodecasubstituted porphyrins.<sup>4,5,14,20</sup> The parameters for cobalt(II) are those determined recently.<sup>5</sup> For the present work, the force field was slightly modified by the use of an exponential-<sup>6</sup> van der Waals potential energy function for the H atoms instead of the Lennard-Jones 12–6 potential. The exponential-6 potential is softer at short interatomic distances, giving a better representation of the nonbonding interaction. Also, accurate predictions of relative energies of porphyrin conformers requires the inclusion of electrostatic terms. Partial atomic charges were obtained using the charge equilibration method.<sup>33e</sup> Although these changes to the force field have recently been shown to give more accurate relative conformational energies,<sup>35</sup> a comparison of porphyrin structures calculated without charges and using the Lennard-Jones 12–6 potential on the hydrogen atoms to structures obtained with charges and exponential-<sup>6</sup> van der Waals potential energy function found no significant structural differences for the porphyrin macrocycle or for the orientation of the substituents relative to one another. Thus, proton geometric factors reported below were obtained using the original form of the porphyrin force field.<sup>4</sup>

(25) For reviews of porphyrins as oxidation catalysts, see: (a) Gunter, M. J.; Turner, P. *Coord. Chem. Rev.* **1991**, *108*, 115. (b) Meunier, B. *Chem. Rev.* **1992**, *92*, 1411. (c) Collman, J. P.; Zhang, X.; Lee, V. J.; Uffelman, E. S.; Brauman, J. I. *Science* **1993**, *261*, 1404.  
 (26) For a review and some current research in this area, see: Walker, F. A.; et al., *New. J. Chem.* **1992**, *16*, 609.  
 (27) Scheidt, W. R.; Chipman, D. M. *J. Am. Chem. Soc.* **1986**, *108*, 1163.  
 (28) Nakamura, M.; Groves, J. T. *Tetrahedron Lett.* **1988**, *44*, 3225.  
 (29) (a) Safo, M. K.; Scheidt, W. R.; Gupta, G. P. *Inorg. Chem.* **1990**, *29*, 626. (b) Hatano, K.; Safo, M. K.; Walker, F. A.; Scheidt, W. R. *Inorg. Chem.* **1991**, *30*, 1643. (c) Safo, M. K.; Gupta, G. P.; Walker, F. A.; Scheidt, W. R. *J. Am. Chem. Soc.* **1991**, *113*, 5497.  
 (30) (a) Zhang, H.; Simonis, U.; Walker, F. A. *J. Am. Chem. Soc.* **1990**, *112*, 6124. (b) Walker, F. A.; Simonis, U. *J. Am. Chem. Soc.* **1991**, *113*, 8652.

(31) Buchler, J. W. In *Porphyrins and Metalloporphyrins*; Smith, K. M., Ed.; Elsevier: Amsterdam, 1975; Chapter 5, p 179.

(32) van Geet, A. L. *Anal. Chem.* **1970**, *42*, 679.

(33) (a) Abe, M.; Kitagawa, T.; Kyogoku, Y. *J. Chem. Phys.* **1978**, *69*, 4526. (b) Li, X.-Y.; Czernuszewicz, R. S.; Kincaid, J. R.; Spiro, T. G. *J. Am. Chem. Soc.* **1989**, *111*, 7012. (c) Li, X.-Y.; Czernuszewicz, R. S.; Kincaid, J. R.; Stein, P.; Spiro, T. G. *J. Chem. Phys.* **1990**, *94*, 47. (d) Mayo, S. L.; Olafson, B. D.; Goddard, W. A. *J. Phys. Chem.* **1990**, *94*, 88. (e) Rappé, A. K.; Goddard, W. A., III. *J. Phys. Chem.* **1991**, *95*, 3358.

(34) Brennan, T. D.; Scheidt, W. R.; Shelnut, J. A. *J. Am. Chem. Soc.* **1988**, *110*, 3919.

(35) Hobbs, J. D.; Majumder, S. A.; Luo, L.; Sickel-Smith, G. A.; Quirke, J. M. E.; Medforth, C. J.; Smith, K. M.; Shelnut, J. A. *J. Am. Chem. Soc.* **1994**, *116*, 3261.

**Table 1.** Calculated Structural Parameters and Energies for Co1a–c, Co3, and Co6a–c Obtained with the Force Field Described in the Experimental Section<sup>a</sup>

porphyrin conformer	energy (kcal mol <sup>-1</sup> )	N–Co–N <sup>38</sup> (deg)	C <sub>α</sub> –N–N–C <sub>α</sub> <sup>37</sup> (deg)
Co1a*	315.5	165.0	0.1
Co1b *ax	386.8	163.5	0.0
Co1b ax–eq <sup>b</sup>	387.7	164.2	3.2
Co1b *eq	393.6	164.1	9.2
Co1c *axial	381.7	163.5	0.8
Co1c ax–eq <sup>b</sup>	382.8	164.1	3.0
Co1c equatorial	406.5	166.2	21.6
Co3*	518.6	165.6	2.2
Co6a*	471.9	180.0	0.1
Co6b *form A	347.9	169.5	19.7
Co6b form B	350.3	167.8	0.5
Co6c *eq chairs	375.7	163.8	0.1
Co6c 2ax/2 eq (trans)	378.1	162.7	0.1
Co6c *ax chairs	380.6	161.6	0.1
Co6c eq boats	397.0	164.2	0.1
Co6c ax boats	397.5	162.6	0.4

<sup>a</sup> Structures marked with an asterisk are shown in Figures 2 and 3. Ax = axial and eq = equatorial. <sup>b</sup> One alkyl group on each pyrrole ring is axial; the other alkyl group is equatorial.

## Results and Discussion

**Molecular Mechanics Calculations.** A molecular mechanics force field<sup>4,5</sup> which accurately reproduces the crystal structures of dodecasubstituted porphyrins has been modified as described and used to calculate energy minimized structures for Co1a–c, Co3, and Co6a–c. The influence of different initial orientations of the pyrrole substituents on the calculated energy and conformation of the porphyrin macrocycle was also investigated. Some selected geometric parameters and the total energies for all of the conformers calculated are listed in Table 1.

Minimum energy structures obtained from the molecular mechanics calculations for Co1a–c and Co3 are shown in Figure 2. In all cases the porphyrin macrocycles adopt highly nonplanar saddle<sup>36</sup>, conformations similar to those determined crystallographically for Zn1a,<sup>3b</sup> Zn1b,<sup>3b</sup> Cu1b,<sup>5</sup> Co1b,<sup>5</sup> Ni1b,<sup>7</sup> Ni1c,<sup>7</sup> and free base 3.<sup>14</sup> For Co1b and Co1c, the molecular mechanic calculations also indicate that the lowest energy structures are those with all quasi-axial ethyl or propyl substituents (Table 1). The conformations of the substituents are therefore the same as those determined crystallographically.<sup>3b,5,7</sup> This gives rise to a cavity (or groove) in which the ethyl or propyl groups form the sides of the cavity (Figure 2, top right and bottom left). When the alkyl groups of Co1b are switched into quasi-equatorial positions (Figure 2, top center) the cavity structure is essentially lost. The macrocycle also tends to become more ruffled<sup>36</sup> when the ethyl groups are equatorial, as measured by an increase in the calculated C<sub>α</sub>–N–N–C<sub>α</sub> torsion angles<sup>37</sup> (Table 1) with amount of saddle deformation (as measured by the N–Co–N angle<sup>38</sup>) being essentially unchanged. In the case of Co3, the cavity formed by the pyrrole

phenyl rings is slightly wider than that formed by the axial ethyl or propyl groups of Co1b and Co1c (Figure 2, bottom right).

Figure 3 illustrates how enlarging the fused ring in the series Co6a–c increases the nonplanarity of the porphyrin macrocycle. These results, obtained using the improved force field, generally confirm the previously reported molecular mechanics calculations for this series.<sup>4</sup> Co6a is calculated to be planar (N–Co–N = 180°, C<sub>α</sub>–N–N–C<sub>α</sub> = 0°), which agrees with previous experimental and molecular modeling studies indicating that the five-membered ring significantly decreases the peripheral steric strain responsible for a nonplanar conformation.<sup>4,7,19,20</sup> Crystallographic studies have shown that Cu6a crystallizes in an essentially planar conformation.<sup>20</sup> For Co6b, the larger six-membered ring increases the steric interactions between the peripheral substituents and the macrocycle is nonplanar. The lowest energy conformer of Co6b (designated form A) exhibits both ruffling and saddling deformation (N–Co–N = 169.4°, C<sub>α</sub>–N–N–C<sub>α</sub> = 19.8°), although the crystal structure of Ni6b<sup>7</sup> is closer to the slightly higher energy saddle conformation designated form B. Note that the conformations of the six-membered rings in Co6b do not allow the formation of a well-defined cavity structure (Figure 3, top right).

Co6c has seven-membered rings fused to the pyrrole rings and adopts a saddle structure that is more nonplanar than that of Co6b (Table 1). The calculated increase in nonplanarity for Co6c is consistent with spectroscopic studies of porphyrins 6b,c.<sup>4,19,20</sup> The calculations indicate that the degree of nonplanarity does not change much if the seven-membered ring is in a boat or a chair conformation or if the ring is in quasi-axial or quasi-equatorial positions (Table 1). The calculations also show that an equatorial chair conformation of the seven-membered ring is favored. Note that an axial chair conformation of the seven-membered ring gives the porphyrin a well-defined cavity structure but an equatorial chair conformation does not (Figure 3, bottom). A preliminary crystal structure of Ni6c shows a nonplanar saddle structure with a mixture of axial and equatorial chair conformations of the seven-membered ring.<sup>39</sup>

**Solution Conformations Determined from Cobalt(II) Paramagnetic Shifts.** In low-spin cobalt(II) porphyrins the observed paramagnetic shifts are predominantly dipolar in nature.<sup>40a</sup> Structural information can therefore be obtained by comparing the observed paramagnetic shifts with dipolar shifts calculated from the geometric factors of protons in the molecule.<sup>40</sup> The molecular mechanics structures of Co1a–c, Co3, and Co6a–c and the crystal structure of Co1b<sup>5</sup> are used to calculate these geometric factors ( $1 - 3(\cos^2 \theta)/r^3$ ) for each proton based on its location ( $r, \theta$ ) in the dipolar field of the unpaired spin on the Co(II) ion. For this calculation,  $r$  is the

(36) The nomenclature used to describe nonplanar conformations is taken from: Scheidt, W. R.; Lee, Y. J. *Struct. Bonding* **1987**, *64*, 1. In a saddle conformation, alternate pyrrole rings are tilted up and down with respect to a least-squares plane through the 24 atoms of the porphyrin core. The meso atoms remain in the least-squares plane. In a ruffled conformation alternate pyrrole rings are twisted clockwise or anticlockwise about the M–N bond such that the meso carbon atoms are alternately above or below the least-squares plane through the 24 atoms of the porphyrin core.

(37) The degree of pyrrole twisting or porphyrin ruffling can be defined by the torsion angle between the  $\alpha$ -carbon and nitrogen atom of a pyrrole ring and the nitrogen atom and  $\alpha$ -carbon of the opposite pyrrole ring. The C<sub>α</sub>–N–N–C<sub>α</sub> angle is 0° for a planar porphyrin or a pure saddle structure.

(38) For an in-plane metal atom the degree of pyrrole tilting or porphyrin saddle distortion can be defined by the angle formed between a pyrrole nitrogen atom, the metal atom, and an opposite nitrogen atom. The N–M–N angle is 0° for a planar structure or a pure ruffled structure.

(39) A preliminary analysis of the crystal structure of Ni6c yields three independent porphyrin molecules in the unit cell. The porphyrin macrocycles adopt very nonplanar saddle conformations, and the seven-membered rings display either axial or equatorial chair conformations. Some disorder of the seven-membered rings is also present. Barkigia, K. M. Personal communication.

(40) (a) LaMar, G. N.; Walker, F. A. In *The Porphyrins*; Dolphin, D., Ed.; Academic Press: New York, 1979; Vol. 4, pp 119–126. (b) *NMR of Paramagnetic Molecules: Principles and Applications*; La Mar, G. N., Horrocks, W. DeW., Holms, R. H., Eds.; Academic Press: New York, 1973. (c) *NMR of Paramagnetic Molecules in Biological Systems*; Bertini, I., Luchinat, C., Eds.; Benjamin/Cummings: Menlo Park, CA, 1986. (d) Clayden, N. J.; Moore, G. R.; Williams, G. *Met. Ions Biol. Syst.* **1987**, *21*, 187. (e) Clayden, N. J.; Moore, G. R.; Williams, R. J. P.; Baldwin, J. E.; Crossley, M. J. *J. Chem. Soc., Perkin Trans.* **1983**, 1863. (f) Botuliniski, A.; Buchler, J. W.; Tonn, B.; Wicholas, M. *Inorg. Chem.* **1985**, *24*, 3239. (g) Abraham, R. J.; Marsden, I.; Xiuqing, L. *Magn. Reson. Chem.* **1990**, *28*, 1051.



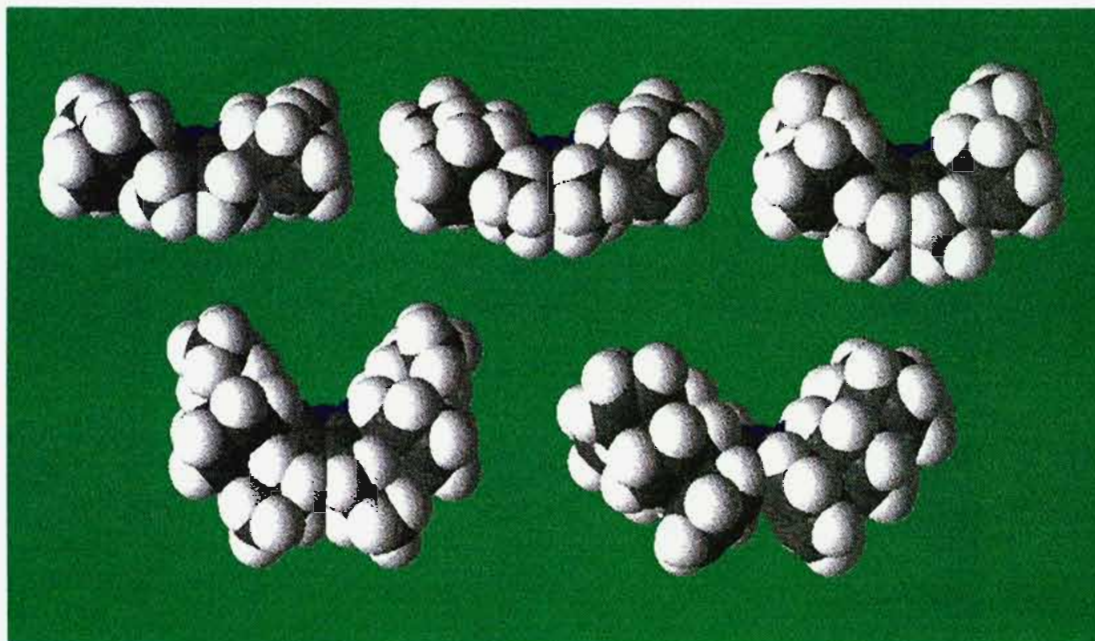


**Figure 2.** Space-filling models of minimum energy structures obtained with the force field described in the Experimental Section. Top from left to right: Co1a; Co1b with equatorial ethyl groups; Co1b with axial ethyl groups (same conformation of ethyls seen in the crystal structure of Co1b<sup>5</sup>). Bottom from left to right: Co1c with axial propyl groups (same conformation of propyls seen in the crystal structure of Ni1c<sup>7</sup>); Co3.

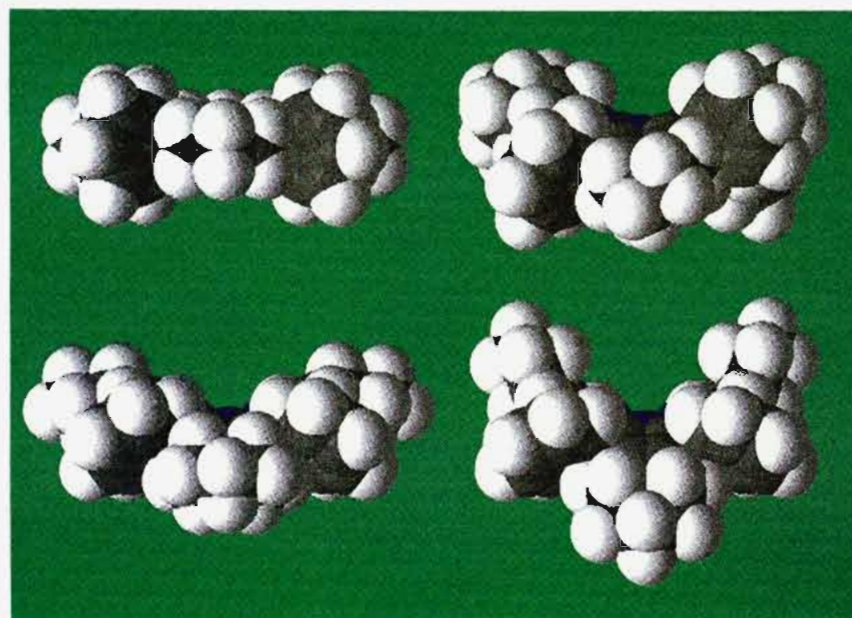


**Figure 3.** Space-filling models of minimum energy structures obtained with the force field described in the Experimental Section. Top from left to right: Co6a; Co6b (form A). Bottom from left to right: Co6c with equatorial chairs; Co6c with axial chairs. For clarity the methoxy groups of Co6a have been omitted.

distance of the proton from the cobalt(II) atom and  $\theta$  is the angle defined by the proton, the cobalt(II) atom, and the  $z$  axis representing the  $d_{z^2}$  orbital where the unpaired electron is localized. The geometric factors were averaged for equivalent groups of protons in the molecule and then normalized<sup>41</sup> by making the  $H_{ortho}$  geometric factor equal to 10.00 (Table 5).

A proton NMR spectrum of one of the nonplanar cobalt(II) porphyrins is shown in Figure 4. The spectrum is similar to the spectra normally observed for planar low-spin cobalt(II) porphyrins.<sup>40a,g</sup> The paramagnetic shifts for the cobalt(II) porphyrins were determined from the proton shifts of the cobalt(II) complexes (Table 2) and the corresponding diamagnetic nickel(II) porphyrin reference compounds (Table 3). Diaste-

reotopic methylene protons were observed in some cases, so to be consistent, the chemical shifts of these protons were averaged for both the cobalt(II) and nickel(II) porphyrins. The paramagnetic shifts measured in this manner for two solvent systems,  $CDCl_3$  or  $C_6D_6$ , are summarized in Table 4. The normalized experimental paramagnetic shifts and the calculated geometric factors (dipolar shifts) for the cobalt(II) porphyrins are summarized in Table 5.

The data in Table 5 are used to investigate the solution structures of the dodecasubstituted porphyrins. For Co1a–c, the paramagnetic shifts of the phenyl protons ( $H_{ortho}$ ,  $H_{meta}$ ,  $H_{para}$ ) are in good agreement with the geometric factors, confirming that the shifts are predominantly dipolar in nature and that the solution structures are similar to the calculated structures. The

(41) LaMar, G. N.; Walker, F. A. *J. Am. Chem. Soc.* 1973, 95, 1790.

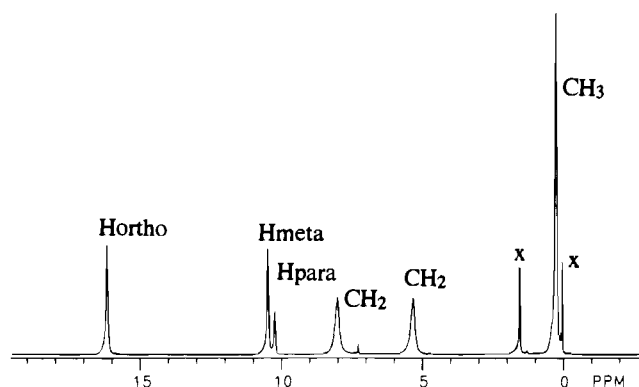


**Figure 4.** 300 MHz proton NMR spectrum of Co1b in CDCl<sub>3</sub> (x = solvent or trace impurity).

**Table 2.** Proton Chemical Shifts ( $\delta_{\text{Co}}$ , ppm) for Cobalt(II) Complexes of Porphyrins 1a–c, 3, and 6a–c

(a) In CDCl <sub>3</sub>								
	Co1a	Co1b	Co1c	Co3	Co6a	Co6b	Co6c	CoTPP <sup>40g</sup>
H <sub>ortho</sub>	16.57	16.13	16.22	12.43	13.12	15.60	17.22	13.16
H <sub>meta</sub>	10.59	10.43	10.50	8.56	5.00	10.42	10.52	9.96
H <sub>para</sub>	10.36	10.19	10.27	8.56	5.80	10.17	10.38	9.75
H <sub>S1</sub>	9.81	7.96	7.92	9.11	9.67	12.13	10.45	15.98
		5.28	5.01				8.23	
H <sub>S2</sub>		0.21	1.66	7.62	5.00	3.11	4.68	
			-0.87				2.16	
H <sub>S3</sub>			0.37	7.98			4.04	
							2.16	

(b) In C <sub>6</sub> D <sub>6</sub>								
	Co1a	Co1b	Co1c	Co3	Co6a	Co6b	Co6c	CoTPP
H <sub>ortho</sub>	16.83	17.33	17.45	14.48	14.06	15.63	18.05	13.09
H <sub>meta</sub>	10.55	10.64	10.69	9.19	4.73	10.36	10.77	9.67
H <sub>para</sub>	10.21	10.30	10.31	9.11	5.99	10.02	10.42	9.45
H <sub>S1</sub>	8.11	10.07	10.42	9.37	13.24	9.55	10.32	16.16
		6.13	6.05				6.49	
H <sub>S2</sub>		0.27	1.95	7.69	5.16	3.45	5.44	
			-0.87				1.95	
H <sub>S3</sub>			0.12	7.98			4.18	
							1.95	

**Table 3.** Proton Chemical Shifts ( $\delta_{\text{Ni}}$ , ppm) for Nickel(II) Complexes of Porphyrins 1a–c, 3, and 6a–c

(a) In CDCl <sub>3</sub> (CD <sub>2</sub> Cl <sub>2</sub> )								
	Ni1a	Ni1b	Ni1c	Ni3	Ni6a	Ni6b	Ni6c	NiTPP
H <sub>ortho</sub>	8.02	8.09	8.02	7.01	7.05	7.87	7.99	8.01
H <sub>meta</sub>	7.65	7.60	7.62	6.51	3.83	7.61	7.65	7.68
H <sub>para</sub>	7.65	7.67	7.68	6.65	4.00	7.61	7.65	7.68
H <sub>S1</sub>	1.80	2.23	2.32	6.65	2.93	2.24	2.13	8.74
			1.77					
H <sub>S2</sub>		0.55	0.82	6.65	2.40	1.44	1.33	
H <sub>S3</sub>			0.38	6.65			1.62	

(b) In C <sub>6</sub> D <sub>6</sub>								
	Ni1a	Ni1b	Ni1c	Ni3	Ni6a	Ni6b	Ni6c	NiTPP
H <sub>ortho</sub>	7.90	8.09	8.07	7.17	7.04	7.84	8.04	7.92
H <sub>meta</sub>	7.35	7.34	7.35	6.57	3.37	7.34	7.44	7.39
H <sub>para</sub>	7.35	7.34	7.35	6.74	4.10	7.34	7.39	7.39
H <sub>S1</sub>	1.99	2.62	2.61	6.91	3.15	2.50	2.41	8.84
		2.15	2.10					
H <sub>S2</sub>		0.52	0.93	6.74	2.34	1.48	1.46	
H <sub>S3</sub>			0.43	6.74			1.62	

paramagnetic shifts for the alkyl substituents, particularly S<sub>2</sub> (substituent carbon 2, methyl) protons of Co1b and the S<sub>2</sub> (methylene) protons of Co1c, agree with the geometric factors calculated for the axial alkyl groups but not with those calculated for the equatorial alkyl groups. This is consistent with the molecular mechanics calculations which showed that the all axial

**Table 4.** Proton Paramagnetic Shifts ( $\delta_{\text{Co}} - \delta_{\text{Ni}}$ , ppm) for Porphyrins 1a–c, 3, and 6a–c

(a) In CDCl <sub>3</sub>								
	Co1a	Co1b	Co1c	Co3	Co6a	Co6b	Co6c	CoTPP
H <sub>ortho</sub>	8.55	8.04	8.20	5.42	6.07	7.73	9.23	5.15
H <sub>meta</sub>	2.94	2.83	2.88	2.01	1.17	2.81	2.87	2.28
H <sub>para</sub>	2.71	2.52	2.59	1.91	1.80	2.56	2.73	2.07
H <sub>S1</sub>	8.01	4.39	4.42	2.46	6.74	9.89	7.21	7.24
H <sub>S2</sub>		-0.34	-0.43	0.97	2.60	1.67	2.09	
H <sub>S3</sub>			-0.01	1.33			1.48	

(b) In C <sub>6</sub> D <sub>6</sub>								
	Co1a	Co1b	Co1c	Co3	Co6a	Co6b	Co6c	CoTPP
H <sub>ortho</sub>	8.93	9.24	9.38	7.31	7.02	7.79	10.01	5.17
H <sub>meta</sub>	3.20	3.30	3.34	2.62	1.36	3.02	3.43	2.28
H <sub>para</sub>	2.86	2.96	2.96	2.37	1.89	2.68	3.08	2.06
H <sub>S1</sub>	6.12	5.72	5.88	2.46	10.09	7.05	6.00	7.32
H <sub>S2</sub>		-0.25	-0.39	0.95	2.82	1.97	2.24	
H <sub>S3</sub>			-0.31	1.24			1.45	

conformations of these porphyrins are the minimum energy conformers. The agreement between the geometric factors calculated for Co1b using the molecular mechanics structure and the crystal structure<sup>5</sup> is excellent. The paramagnetic shifts for Co3 also agree reasonably well with the calculated geometric ratios. However, the geometric factors for the S<sub>1</sub> protons in Co3 (the phenyl ortho protons) are closer to the shifts in C<sub>6</sub>D<sub>6</sub> rather than the shifts in CDCl<sub>3</sub>, an effect which is also seen for the S<sub>1</sub> protons of Co1a–c. This suggests that the paramagnetic shifts measured in CDCl<sub>3</sub> contain greater contact contributions than the shifts measured in C<sub>6</sub>D<sub>6</sub>. The solvent dependence of the paramagnetic shifts in planar and nonplanar porphyrins is examined in more detail below.

For porphyrins Co6a–c which have alkyl rings fused to the pyrrole rings, the agreement between the geometric factors and paramagnetic shifts is somewhat varied. The geometric factors for the phenyl and S<sub>1</sub> protons in Co6a are in reasonable agreement with the observed shifts, whereas for the S<sub>2</sub> protons the agreement is poor. The agreement was worse when the moderately nonplanar X-ray structure of Ni6a<sup>20</sup> was used to calculate the geometric factors. One reason for the slightly poorer agreement between the observed and calculated shifts for Co6a could be the fluxional motions of the porphyrin or the pseudorotation of the five-membered ring which is not taken into account by this static model. Turning to Co6b, good agreement is found between the paramagnetic shifts measured in C<sub>6</sub>D<sub>6</sub> and the geometric ratios calculated for the form B molecular mechanics structure, which is also similar to the saddle structure determined crystallographically for Ni6b.<sup>7</sup> For Co6c, the geometric factors calculated for the phenyl protons of the equatorial and axial chair structures agree fairly well with the observed shifts, although the paramagnetic shifts for the methylene protons of the seven-membered rings do not fit well with the geometric factors calculated for either the axial chair conformations or the equatorial chair conformations. The methylene shifts do correspond almost exactly to an average of the geometric factors for axial and equatorial environments, suggesting that the seven-membered rings are present as a mixture of axial and equatorial chair forms in solution. This observation is consistent with preliminary crystallographic data for Ni6c.<sup>39</sup>

#### Variable-Temperature NMR Studies of Co1b and Co6c.

A novel macrocyclic inversion process has previously been detected in variable-temperature NMR studies of several dodecasubstituted porphyrins.<sup>3b,13,14,19,20</sup> Consequently, variable-temperature NMR spectroscopy was used to determine whether macrocyclic inversion and other dynamic processes could be

**Table 5.** Normalized Paramagnetic Shifts and Geometric Factors for Co1a–c, Co3, and Co6a–c<sup>a</sup>

	aryl protons			protons on substituent carbon no.		
	H <sub>ortho</sub>	H <sub>meta</sub>	H <sub>para</sub>	S1	S2	S3
<b>Co1a</b>						
calc	10.00	4.00	3.16	6.34		
obs (CDCl <sub>3</sub> )	10.00	3.44	3.17	9.37		
obs (C <sub>6</sub> D <sub>6</sub> )	10.00	3.58	3.20	6.85		
<b>Co1b</b>						
calc (cryst data <sup>5</sup> )	10.00	4.06	3.28	7.35	-1.12	
calc (all ax)	10.00	4.09	3.33	7.22	-0.85	
calc (ax–eq, ax) <sup>b</sup>	10.00	4.07	3.29	7.20	-0.46	
calc (ax–eq, eq) <sup>b</sup>	10.00	4.07	3.29	5.22	+6.08	
obs (CDCl <sub>3</sub> )	10.00	3.52	3.13	5.46	-0.42	
obs (C <sub>6</sub> D <sub>6</sub> )	10.00	3.57	3.20	6.19	-0.27	
<b>Co1c</b>						
calc (all ax)	10.00	4.13	3.36	7.36	-0.17	+0.72
calc (ax–eq, ax) <sup>b</sup>	10.00	4.07	3.29	6.49	-3.53	-0.19
calc (ax–eq, eq) <sup>b</sup>	10.00	4.07	3.29	6.05	+7.06	+3.23
obs (CDCl <sub>3</sub> )	10.00	3.51	3.16	5.39	-0.52	-0.01
obs (C <sub>6</sub> D <sub>6</sub> )	10.00	3.56	3.16	6.27	-0.42	-0.33
<b>Co3</b>						
calc	10.00	4.01	3.20	3.29	1.63	1.56
obs (CDCl <sub>3</sub> )	10.00	3.71	3.52	4.54	1.79	2.45
obs (C <sub>6</sub> D <sub>6</sub> )	10.00	3.58	3.24	3.37	1.30	1.70
<b>Co6a</b>						
calc	10.00	2.61	2.87	12.16	7.66	
calc (Ni6a cryst) <sup>20</sup>	10.00	1.75	2.21	15.50	9.14	
obs (CDCl <sub>3</sub> )	10.00	1.93	2.97	11.10	4.28	
obs (C <sub>6</sub> D <sub>6</sub> )	10.00	1.94	2.69	14.37	4.02	
<b>Co6b</b>						
calc (form A)	10.00	4.45	3.90	10.71	4.80	
calc (form B)	10.00	4.39	3.73	9.14	3.31	
obs (CDCl <sub>3</sub> )	10.00	3.64	3.31	12.79	2.16	
obs (C <sub>6</sub> D <sub>6</sub> )	10.00	3.88	3.44	9.05	2.53	
<b>Co6c</b>						
calc (eq chairs)	10.00	3.94	3.12	5.05	5.79	3.07
calc (ax chairs)	10.00	3.79	2.91	6.51	-2.09	0.11
calc (av) <sup>c</sup>	10.00	3.87	3.01	5.80	1.71	1.53
obs (CDCl <sub>3</sub> )	10.00	3.11	2.96	7.81	2.26	1.60
obs (C <sub>6</sub> D <sub>6</sub> )	10.00	3.42	3.08	5.99	2.24	1.45
<b>CoTPP</b>						
calc (90° <sup>d</sup> )	10.00	4.94	4.53	21.53		
calc (65° <sup>d</sup> )	10.00	4.50	3.93	18.64		
obs (CDCl <sub>3</sub> )	10.00	4.43	4.02	14.06		
obs (C <sub>6</sub> D <sub>6</sub> )	10.00	4.41	3.98	14.16		

<sup>a</sup> Unless noted the geometric factors were obtained from molecular mechanics structures. <sup>b</sup> For a conformation with one alkyl group on each pyrrole ring in an equatorial position and the other alkyl group in an axial position. <sup>c</sup> Obtained by averaging geometric factors for conformers with all axial and all equatorial chairs and then normalizing data. <sup>d</sup> The angle given is between the porphyrin and phenyl least-squares planes. Calculated geometric factors are taken from ref 40g.

detected for the Co(II) porphyrins examined. For Co1b in C<sub>6</sub>D<sub>5</sub>-CD<sub>3</sub>, the methylene protons are diastereotopic at room temperature but broaden upon heating and ultimately give a single signal at high temperatures. Using the standard equation<sup>42</sup>  $\Delta G^*_{368\text{ K}}$  was calculated to be  $16.1 \pm 0.3 \text{ kcal mol}^{-1}$ . The dynamic process is similar to those reported previously for macrocyclic inversion in other complexes of porphyrin 1b (e.g., Ni1b:  $\Delta G^*_{293\text{ K}} = 13.2 \pm 0.2 \text{ kcal mol}^{-1}$ ).<sup>3b</sup> This indicates that the cavity structure is fluxional as a result of macrocyclic inversion. When a solution of Co1b was cooled to 184 K in CD<sub>2</sub>Cl<sub>2</sub>, separate signals were not observed for axial and equatorial alkyl groups.<sup>43</sup> This result is consistent with the all

axial structure of Co1b determined previously. However, a small fraction of the ethyl groups could still be in equatorial positions and remain undetected if ethyl rotation was rapid on the NMR time scale at all the temperatures studied.

The methylene protons of Co6c in C<sub>6</sub>D<sub>6</sub> are also diastereotopic at room temperature and coalesce upon warming, which is consistent with macrocyclic inversion occurring for this porphyrin as well.<sup>19,20</sup> The standard equation gives  $\Delta G^*_{323\text{ K}} = 13.8 \pm 0.5 \text{ kcal mol}^{-1}$ . A very complicated spectrum was obtained upon cooling Co6c to low temperatures in CD<sub>2</sub>Cl<sub>2</sub>, possibility indicating multiple conformations of the seven-membered ring. This is consistent with the solution conformation of Co6c obtained from the paramagnetic shifts, as well as the preliminary crystal structure of Ni6c.<sup>39</sup> Two dynamic processes are apparent in the methylene proton region of the 300 MHz proton NMR spectrum of diamagnetic Ni6c (Figure 5). The higher energy process ( $\Delta G^*$  estimated as  $11.6 \pm 0.5 \text{ kcal mol}^{-1}$ ) is consistent with macrocyclic inversion, as only the methylene protons become diastereotopic.<sup>19,20</sup> When the lower energy process ( $\Delta G^* = 9.2 \pm 0.5 \text{ kcal mol}^{-1}$ ) is slow on the NMR time scale, multiple phenyl proton signals and multiple carbon-13 signals are observed, supporting the suggestion that this process interconverts different conformations of the seven-membered rings. Dynamic processes have previously been reported for analogous seven-membered rings in cycloheptene ( $5.0 \text{ kcal mol}^{-1}$ ), 4,4-difluorocycloheptene ( $7.8 \text{ kcal mol}^{-1}$ ), and benzocycloheptene ( $10.9 \text{ kcal mol}^{-1}$ ).<sup>44</sup>

**Formation of  $\pi$ -Complexes with 1,3,5-Trinitrobenzene.** The  $\pi$ -complexes formed by porphyrins and  $\pi$ -donor or  $\pi$ -acceptor molecules have been extensively investigated.<sup>45,46</sup> The structure of the  $\pi$ -complex formed between planar (5,10,15,20-tetra-*p*-tolylporphyrato)cobalt(II) (CoTPP; R = *p*-C<sub>6</sub>H<sub>4</sub>CH<sub>3</sub>, R<sup>1</sup> = H in Figure 1) and 1,3,5-trinitrobenzene (TNB) in CDCl<sub>3</sub> has been well characterized.<sup>46b</sup> We were curious about the effect of nonplanarity and the presence of a cavity on the formation of  $\pi$ -complexes; therefore, the interaction of TNB with both planar and nonplanar Co(II) dodecasubstituted porphyrins was investigated. When TNB is added to the planar Co6a, significant changes in both the porphyrin and TNB resonances are observed (Table 6). These changes are similar to those observed when a  $\pi$ -complex is formed between CoTPP and TNB<sup>46b</sup> and suggest that Co6a and TNB also form a  $\pi$ -complex. A similar pattern of changes is observed for Co6b, although the chemical shifts changes are smaller (Table 6). This is consistent with weaker interaction in the complex for Co6b, which is reasonable given that nonplanarity of the porphyrin macrocycle will tend to disrupt  $\pi$ - $\pi$  interactions. Note that in both Co6a and Co6b the S1 protons experience unusually large chemical shift changes, analogous to the large solvent dependencies noted earlier for these protons. Finally, if TNB is added to Co1b, which is more nonplanar than Co6b and has bulky groups that form a cavity on either face of the porphyrin macrocycle, the

(43) A similar result was obtained when a solution of the dication of 1b was cooled to 183 K in CD<sub>2</sub>Cl<sub>2</sub> and a solution of Ni1c was cooled to 189 K in CD<sub>2</sub>Cl<sub>2</sub>.

(44) Oki, M. *Applications of Dynamic NMR Spectroscopy to Organic Chemistry*; VCH: New York, 1985; p 308.

(45) (a) Hill, H. A. O.; Mann, B. E.; Williams, R. J. P. *J. Chem. Soc., Chem. Commun.* **1967**, 906. (b) Hill, H. A. O.; Sadler, P. J.; Williams, R. J. P. *J. Chem. Soc., Dalton Trans.* **1973**, 1663. (c) Hill, H. A. O.; Sadler, P. J.; Williams, R. J. P.; Barry, C. D. *Ann. N.Y. Acad. Sci.* **1973**, 206, 247. (d) Barry, C. D.; Hill, H. A. O.; Mann, B. E.; Sadler, P. J.; Williams, R. J. P. *J. Am. Chem. Soc.* **1973**, 95, 4545. (e) Barry, C. D.; Hill, H. A. O.; Sadler, P. J.; Williams, R. J. P. *Proc. R. Soc. London, Ser. A* **1973**, 334, 493. (f) Ford, L.; Hill, H. A. O.; Mann, B. E.; Sadler, P. J.; Williams, R. J. P. *Biochim. Biophys. Acta* **1976**, 430, 413.

(46) (a) Fulton, G. P.; LaMar, G. N. *J. Am. Chem. Soc.* **1976**, 99, 2119. (b) Fulton, G. P.; LaMar, G. N. *J. Am. Chem. Soc.* **1976**, 99, 2124.

(42) *Introduction to NMR Spectroscopy*; Abraham, R. J., Fisher, J., Loftus, P., Eds.; Wiley: Chichester, U.K., 1988.



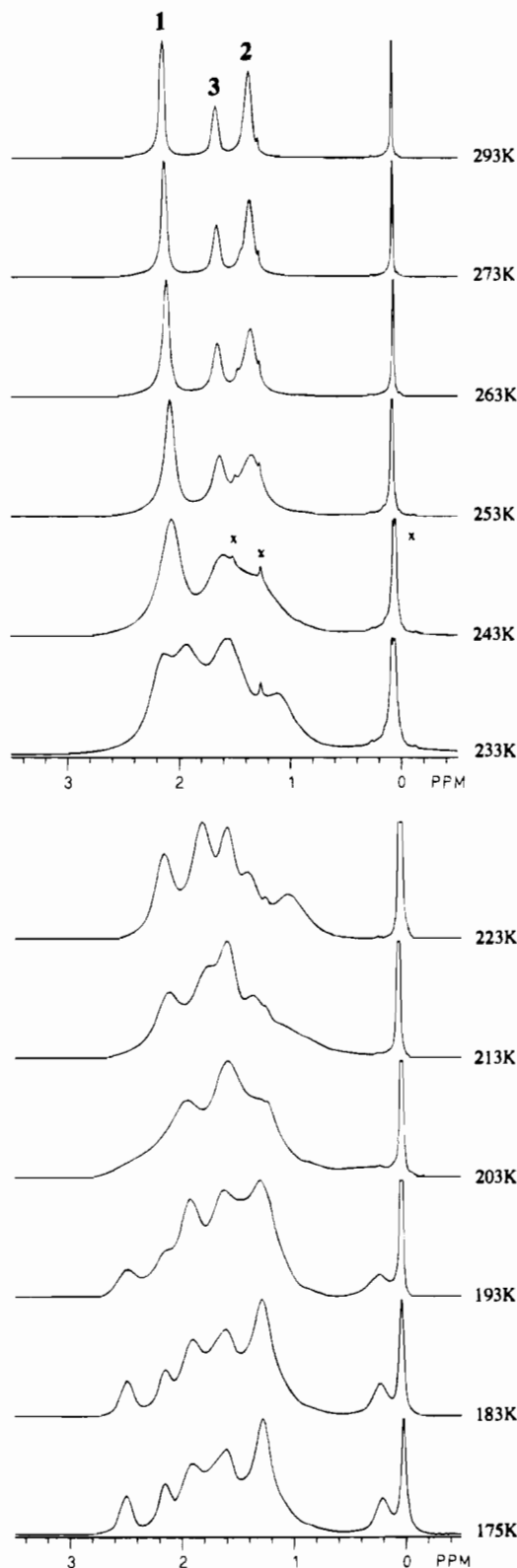


**Figure 5.** Methylene region from the 300 MHz proton NMR spectrum of Ni6c in  $\text{CD}_2\text{Cl}_2/\text{CS}_2$  (1:1) as a function of temperature (x = solvent or trace impurity).

chemical shifts of the porphyrin and TNB protons are independent of the amount of TNB added (Table 6). This shows that the cavity of the nonplanar porphyrin Co1b effectively inhibits  $\pi$ -complex formation.

**Solvent Dependence of the Paramagnetic Shifts.** It has previously been shown that the magnetic anisotropy of cobalt(II) 5,10,15,20-tetraarylporphyrins is markedly decreased by axial solvation in  $\text{CD}_3\text{SOCD}_3$ .<sup>40e</sup> In contrast, similar magnetic

**Table 6.** Chemical Shifts ( $\delta$ , ppm) for Co6a, Co6b, and Co1b in  $\text{CDCl}_3$  as a Function of Trinitrobenzene (TNB) Concentration<sup>a</sup>

	Co6a equiv of TNB			Co6b equiv of TNB					Co1b equiv of TNB	
	0	11	44	0	1	8	27	71	0	62
H <sub>ortho</sub>	13.12	14.22	14.53	15.60	15.61	15.64	15.73	15.85	16.13	16.12
H <sub>meta</sub>	5.00	5.39	5.44	10.42	10.42	10.45	10.53	10.62	10.43	10.44
H <sub>para</sub>	5.80	6.08	6.09	10.17	10.17	10.19	10.26	10.34	10.19	10.20
H <sub>S1</sub>	9.67	14.07	15.06	12.12	12.18	12.46	13.18	14.10	7.96	7.99
H <sub>S2</sub>	5.00	5.17	5.23	3.11	3.13	3.18	3.33	3.50	5.28	5.29
TNB		5.57	8.17		8.76		8.89	9.04		9.39

<sup>a</sup> The chemical shift of TNB in  $\text{CDCl}_3$  is 9.39 ppm.

anisotropies were observed for CoTTP in less polar solvents such as  $\text{CDCl}_3$  and  $\text{C}_6\text{D}_5\text{CD}_3$ .<sup>41</sup> We were interested in determining whether the nonplanarity or cavity structures of some of the dodecasubstituted porphyrins would alter these porphyrin-solvent interactions. Thus, solvent dependences of the proton chemical shifts of CoTTP, Co6a, Co6b, and Co1b were determined. The chemical shifts of CoTTP, Co6a, Co6b, and Co1b in a range of chlorinated solvents, aromatic solvents, and  $\text{CD}_3\text{SOCD}_3$  are given in Table 7. The chemical shifts measured for CoTTP confirm the earlier studies.<sup>40e,41</sup> Large upfield shifts are seen in  $\text{CD}_3\text{SOCD}_3$ , but only small chemical shift differences are seen for the relatively nonpolar chlorinated and aromatic solvents. In fact, a good linear correlation ( $r = 0.99$ ) between the chemical shifts of the H<sub>ortho</sub> and H<sub>pyrrole</sub> protons and the solvent dielectric constant ( $\epsilon$ ) is observed for CoTTP (Table 7), although other measures of solvent polarity do not give a linear relationship. The other protons of CoTTP also correlate with the dielectric constant but with more scatter ( $R^2 = 0.88 - 0.90$ ), probably because their dependences on  $\epsilon$  are weaker. Data for the dodecasubstituted porphyrins show that they behave in essentially the same manner as CoTTP, irrespective of the conformation of the macrocycle. This suggests that even the relative tight cavity structure of Co1b does not significantly inhibit axial solvation. One point of interest in Table 7 is the strong solvent dependence of the normalized paramagnetic shifts for the S1 methylene protons, which was noted earlier. The data presented in Table 7 support the idea that the S1 protons have a significant solvent dependent contact shift.

**Temperature Dependence of the Paramagnetic Shifts.** It is well-known that temperature dependent changes in the structures of paramagnetic molecules can give rise to nonlinear Curie plots.<sup>40a-d</sup> For example, a Curie plot obtained for CoTTP in  $\text{CDCl}_3$  showed significant deviations from linearity at low temperatures.<sup>41</sup> This was explained in terms of greater axial solvation causing an increase in the axial ligand field and, hence, a decrease in the magnetic anisotropy. Curie plots were determined for Co6a, Co6b, and Co1b in  $\text{CD}_2\text{Cl}_2$  (Figure 6) and  $\text{C}_6\text{D}_5\text{CD}_3$  over the usable temperature ranges of these solvents to see if the dodecasubstituted porphyrins behaved in a similar fashion to CoTTP. With exclusion of the anomalous S1 protons, which show significant deviations from nonlinearity as well as non-zero intercepts, the Curie plots generally had zero intercepts and were linear or showed some deviation from linearity at low temperatures. The plots also typically became more linear in the series Co6a < Co6b < Co1b (in  $\text{CD}_2\text{Cl}_2$ , Figure 6). It is not possible at this time to give a precise description of the temperature dependence of the paramagnetic shifts in these porphyrins. However, the more linear Curie plots for Co1b are reasonable given that the conformation of this highly nonplanar porphyrin may be less temperature dependent and the cobalt(II) ion slightly more difficult to solvate.

**Table 7.** Solvent Dependence of the Chemical Shifts ( $\delta$ , ppm) of Co**1b**, Co**6a**, Co**6b**, and CoTPP with Normalized Paramagnetic Shifts in Parentheses<sup>a</sup>

CoTPP						
	H <sub>ortho</sub>	H <sub>meta</sub>	H <sub>para</sub>	H <sub>pyrrole</sub>	$\epsilon$ at 20 °C	
C <sub>6</sub> D <sub>6</sub>	13.09 (10.00)	9.67 (4.41)	9.45 (3.98)	16.16 (14.16)	2.28	
C <sub>6</sub> D <sub>5</sub> CD <sub>3</sub>	13.03 (10.00)	9.68 (4.48)	9.45 (4.03)	16.04 (14.09)	2.38	
CCl <sub>4</sub>	13.41 (10.00)	9.99 (4.28)	9.76 (3.85)	16.21 (13.81)	2.24	
CDCl <sub>3</sub>	13.16 (10.00)	9.96 (4.43)	9.75 (4.02)	15.98 (14.06)	4.81	
CD <sub>2</sub> Cl <sub>2</sub>	12.86 (10.00)	9.84 (4.45)	9.63 (4.02)	15.55 (14.05)	8.93	
CDCl <sub>2</sub> CDCl <sub>2</sub>	12.54 (10.00)	9.68 (4.42)	9.48 (3.97)	15.31 (14.50)	9 <sup>c</sup>	
CD <sub>3</sub> SOCD <sub>3</sub>	9.38 (10.00)	8.68 (7.30)	8.31 (4.60)	12.71 (28.98)	46.68	
Co <b>6a</b>						
	H <sub>ortho</sub>	H <sub>meta</sub>	H <sub>para</sub>	H <sub>S1</sub>	H <sub>S2</sub>	$\epsilon$ at 20 °C
C <sub>6</sub> D <sub>6</sub>	14.06 (10.00)	4.73 (1.94)	5.99 (2.69)	13.24 (14.37)	5.16 (4.02)	2.28
C <sub>6</sub> D <sub>5</sub> CD <sub>3</sub>	13.97 (10.00)	4.77 (2.02)	5.92 (2.63)	12.56 (13.58)	5.13 (4.03)	2.38
CCl <sub>4</sub>	13.47 (10.00)	5.10 (1.98)	5.79 (2.79)	10.68 (12.07)	5.28 (4.49)	2.24
CDCl <sub>3</sub>	13.12 (10.00)	5.00 (1.93)	5.80 (2.97)	9.67 (11.10)	5.00 (4.28)	4.81
CD <sub>2</sub> Cl <sub>2</sub>	12.67 (10.00)	4.89 (1.89)	5.59 (2.83)	8.96 (10.73)	4.72 (4.13)	8.93
CDCl <sub>2</sub> CDCl <sub>2</sub>	11.93 (10.00)	4.71 (1.80)	5.41 (2.89)	7.31 (8.98)	4.47 (4.24)	9 <sup>c</sup>
CD <sub>3</sub> SOCD <sub>3</sub>	8.74 (10.00)	4.23 (2.37)	4.53 (3.14)	<i>b</i>	3.19 (4.67)	46.68
Co <b>6b</b>						
	H <sub>ortho</sub>	H <sub>meta</sub>	H <sub>para</sub>	H <sub>S1</sub>	H <sub>S2</sub>	$\epsilon$ at 20 °C
C <sub>6</sub> D <sub>6</sub>	15.63 (10.00)	10.36 (3.88)	10.02 (3.44)	9.55 (9.05)	3.45 (2.53)	2.28
C <sub>6</sub> D <sub>5</sub> CD <sub>3</sub>	15.53 (10.00)	10.34 (3.90)	10.01 (3.47)	9.41 (8.99)	3.56 (2.70)	2.38
CCl <sub>4</sub>	15.78 (10.00)	10.58 (3.75)	10.23 (3.30)	8.74 (8.22)	3.32 (2.38)	2.24
CDCl <sub>3</sub>	15.60 (10.00)	10.42 (3.64)	10.17 (3.31)	12.13 (12.79)	3.11 (2.16)	4.81
CD <sub>2</sub> Cl <sub>2</sub>	15.59 (10.00)	10.52 (3.77)	10.24 (3.41)	12.37 (13.12)	3.37 (2.50)	8.93
CDCl <sub>2</sub> CDCl <sub>2</sub>	14.56 (10.00)	10.07 (3.68)	9.84 (3.33)	9.22 (10.43)	3.03 (2.38)	9 <sup>c</sup>
CD <sub>3</sub> SOCD <sub>3</sub>	10.30 (10.00)	8.89 (5.27)	8.61 (4.12)	<i>b</i>	2.03 (2.43)	46.68
Co <b>1b</b>						
	H <sub>ortho</sub>	H <sub>meta</sub>	H <sub>para</sub>	H <sub>S1</sub>	H <sub>S2</sub>	$\epsilon$ at 20 °C
C <sub>6</sub> D <sub>6</sub>	17.33 (10.00)	10.64 (3.57)	10.30 (3.20)	10.07/6.13 (6.19)	0.27 (-0.27)	2.28
C <sub>6</sub> D <sub>5</sub> CD <sub>3</sub>	17.10 (10.00)	10.57 (3.58)	10.24 (3.22)	9.31/5.89 (5.78)	0.29 (-0.26)	2.38
CCl <sub>4</sub>	16.86 (10.00)	10.65 (3.48)	10.34 (3.04)	8.39/5.26 (5.24)	0.12 (-0.49)	2.24
CDCl <sub>3</sub>	16.13 (10.00)	10.43 (3.52)	10.19 (3.13)	7.96/5.28 (5.46)	0.21 (-0.42)	4.81
CD <sub>2</sub> Cl <sub>2</sub>	16.45 (10.00)	10.53 (3.50)	10.30 (3.15)	9.20/5.36 (6.04)	-0.08 (-0.75)	8.93
CDCl <sub>2</sub> CDCl <sub>2</sub>	15.37 (10.00)	10.11 (3.44)	9.95 (3.12)	6.30/4.68 (4.16)	0.31 (-0.33)	9 <sup>c</sup>
CD <sub>3</sub> SOCD <sub>3</sub>	11.20 (10.00)	9.06 (4.69)	8.80 (3.63)	<i>b</i>	0.31 (-0.77)	46.68

<sup>a</sup> Ni(II) complexes in C<sub>6</sub>D<sub>6</sub> used as reference compounds for C<sub>6</sub>D<sub>6</sub> and C<sub>6</sub>D<sub>5</sub>CD<sub>3</sub> solutions; Ni(II) complexes in CDCl<sub>3</sub> or CD<sub>2</sub>Cl<sub>2</sub> used as reference compounds for CCl<sub>4</sub>, CDCl<sub>3</sub>, CD<sub>2</sub>Cl<sub>2</sub>, CDCl<sub>2</sub>CDCl<sub>2</sub>, and CD<sub>3</sub>SOCD<sub>3</sub> solutions (Table 3). <sup>b</sup> Signal is too broad to be measured. <sup>c</sup> Average of two methylene protons. <sup>d</sup> Dielectric constants taken from: *CRC Handbook of Chemistry and Physics, Chem. Phys.*, 71st ed.; Lide, D. R., Ed.; CRC Press: Boca Raton, FL, 1990; p 9-9. <sup>e</sup> Estimated from  $\epsilon$  for 1,1,2,2-tetrabromoethane and *cis*-1,2-dibromo- and dichloroethylene.

## Conclusions

The results presented here show that the solution conformations of the macrocycles and substituents of nonplanar dodecasubstituted porphyrins are similar to those determined crystallographically. Further, molecular mechanics calculations using a force field based upon the normal coordinate analysis and crystal structure of a planar porphyrin can predict the conformer having the lowest energy (global minimum). Initial studies of TNB  $\pi$ - $\pi$  complex formation indicate that the novel structure of porphyrin **1b** significantly influences the interactions of this porphyrin with small molecules. Porphyrins such as **1b** might therefore be effective in modulating other porphyrin-substrate interactions, potentially making them useful as regio- and stereoselective oxidation catalysts,<sup>25</sup> and in the preparation of complexes with well-defined ligand orientations.<sup>26-30</sup> The latter proposal has recently been investigated, and preliminary NMR results indicate that pyridine and imidazole ligands complexed to Co<sup>III</sup>**1b** orient parallel to the cavity formed by the ethyl substituents of the porphyrin.<sup>47</sup> The catalytic activity

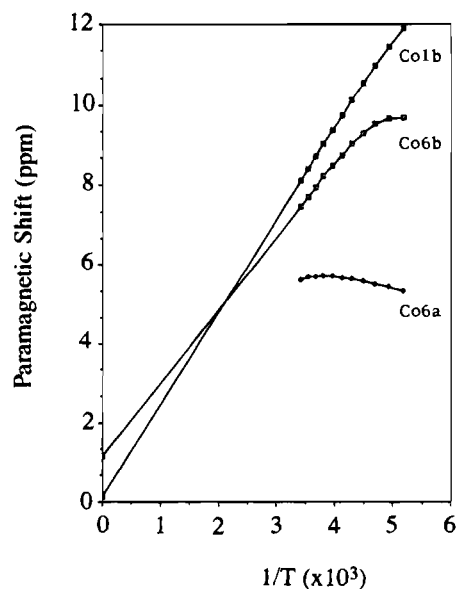


**Figure 6.** Curie plots obtained for the H<sub>ortho</sub> protons of Co**6a**, Co**6b**, and Co**1b** in CD<sub>2</sub>Cl<sub>2</sub>.

(47) Medforth, C. J.; Muzzi, C. M.; Smith, K. M.; Abraham, R. J.; Hobbs, J. D.; Shelnut, J. A. *J. Chem. Soc., Chem. Commun.* **1994**, 1843.



of a wide range of dodecasubstituted iron(III) porphyrins, including fluorinated analogs, is currently under investigation in our laboratories.<sup>48</sup>

**Acknowledgment.** Work performed at the University of California was supported by National Science Foundation Grant CHE-93-05577, National Institutes of Health Grant HL 22252 (K.M.S.), and NATO Grant RG0218 (R.J.A.; K.M.S.). Work

(48) Showalter, M. C.; Medforth, C. J.; Nurco, D. J.; Forsyth, T. P.; Smith, K. M.; Shelnut, J. A. Work in progress.

(49) Munro, O. Q.; Bradley, J. C.; Hancock, R. D.; Marques, H. M.; Marsicano, F.; Wade, P. W. *J. Am. Chem. Soc.* **1992**, *114*, 7218.

performed at Sandia National Laboratories was supported by the U.S. Department of Energy Contract DE-AC04-94DP85000 (J.A.S.). C. J. M. and J.D.H. thank the Associated Western Universities, Inc., for Postdoctoral Fellowships.

**Supplementary Material Available:** Table S1, listing proton chemical shifts for free base porphyrins **1a-c**, **3**, **6a-c**, and tetraphenylporphyrin in CD<sub>2</sub>Cl<sub>2</sub> and C<sub>6</sub>D<sub>6</sub>, and Tables S2-S5, listing calculated structural parameters and energies (kcal mol<sup>-1</sup>) for **Co1a**, **Co1b**, **Co1c**, **Co3**, **Co6a**, **Co6b**, and **Co6c** (5 pages). Ordering information is given on any current masthead page.

IC9403469